AMMRC TR 81-29

MELT PURIFICATION VIA FILTRATION

June 1981

D. APELIAN, R. MUTHARASAN, and C. ROMANOWSKI
College of Engineering
Drexel University
Philadelphia, Pennsylvania 19104

INTERIM REPORT   Contract No. DAAG46-79-C-0052

Prepared for

ARMY MATERIALS AND MECHANICS RESEARCH CENTER
Watertown, Massachusetts 02172

The findings in this report are not to be construed as an official Department of the Army position, unless so designated by other authorized documents.

Mention of any trade names or manufacturers in this report shall not be construed as advertising nor as an official indorsement or approval of such products or companies by the United States Government.

REPORT DOCUMENTATION PAGE		READ INSTRUCTIONS BEFORE COMPLETING FORM
1. REPORT NUMBER AMMRC TR 81-29	2. GOVT ACCESSION NO.	3. RECIPIENT'S CATALOG NUMBER
4. TITLE (and Subtitle) MELT PURIFICATION VIA FILTRATION		5. TYPE OF REPORT & PERIOD COVERED Interim Report - 1 Jan 81 - 1 Apr 81
		6. PERFORMING ORG. REPORT NUMBER
7. AUTHOR(s) D. Apelian, R. Mutharasan, and C. Romanowski		8. CONTRACT OR GRANT NUMBER(s) DAAG46-79-C-0052
9. PERFORMING ORGANIZATION NAME AND ADDRESS College of Engineering Drexel University Philadelphia, Pennsylvania 19104		10. PROGRAM ELEMENT, PROJECT, TASK AREA & WORK UNIT NUMBERS D/A Project: 1L162105AH84 AMCMS Code: 612105.H840011
11. CONTROLLING OFFICE NAME AND ADDRESS Army Materials and Mechanics Research Center ATTN: DRXMR-AP Watertown, Massachusetts 02172		12. REPORT DATE June 1981
		13. NUMBER OF PAGES 42
14. MONITORING AGENCY NAME & ADDRESS(if different from Controlling Office)		15. SECURITY CLASS. (of this report) Unclassified
		15a. DECLASSIFICATION/DOWNGRADING SCHEDULE

16. DISTRIBUTION STATEMENT (of this Report)

Approved for public release; distribution unlimited.

17. DISTRIBUTION STATEMENT (of the abstract entered in Block 20, if different from Report)

18. SUPPLEMENTARY NOTES

19. KEY WORDS (Continue on reverse side if necessary and identify by block number)

Filtration	Steel
Liquid metals	Superalloys
Aluminum	Purification

20. ABSTRACT (Continue on reverse side if necessary and identify by block number)

    Background on the mechanisms and kinetics of filtration is discussed and the Drexel mathematical model is further elaborated and updated to encompass filtration at the higher temperatures encountered in steels and superalloys. A novel mathematical analysis of inclusion trajectory is also presented.

    The aluminum–TiB_2 study has been extended to evaluate a ceramic foam filter. A low temperature model study of liquid inclusion filtration is described and discussed.

    Reference is made to ongoing work in superalloy and steel filtration,

DD FORM 1473   EDITION OF 1 NOV 65 IS OBSOLETE
1 JAN 73

Block No. 20

counter-current gas filtration, filter characterization and flow
visualization.

ABSTRACT

Background on the mechanisms and kinetics of filtration is discussed and the Drexel mathematical model is further elaborated and updated to encompass filtration at the higher temperatures encountered in steels and superalloys. A novel mathematical analysis of inclusion trajectory is also presented.

The aluminum-TiB_2 study has been extended to evaluated a ceramic foam filter. A low temperature model study of liquid inclusion filtration is described and discussed.

Reference is made to ongoing work in superalloy and steel filtration, counter-current gas filtration, filter characterization and flow visualization.

FOREWORD

This is the third semi-annual report prepared by Drexel University. It summarizes the progress made during the period July 1st 1980 to December 31st 1980 on assessing the feasibility of inclusion removal from molten metal systems. The contract DAAG46-79-C0052 is administered under the direction of Mr. Arthur Ayvazian, of the U. S. Army Materials and Mechanics Research Center, Watertown, Massachusetts.

TABLE OF CONTENTS

1. INTRODUCTION

The objective of this work is to characterize, improve and develop molten metal filtering techniques, with particular reference to the feasibility of purifying aluminum, steel and metal based superalloys.

Filtering liquid metals removes impurities present in the melt either as solid or liquid particles. The presence of these particles is known to reduce the fluidity of the melt, cause internal porosity in castings, reduce mechanical strength, ductility and fatigue resistance of the product and also result in poor machinability, surface finish, etc. (1-8).

Until very recently the technology to filter at the elevated temperatures required for steel and superalloys has not been available; however, advances in ceramics, in combination with the need for greater product confidence, has generated a strong interest in the feasibility of such melt purification. This interest is largely confined to superalloys and high cost special steels, e.g., razor blade steel; however, the prospect of developing a low cost filtration process for normal high tonnage carbon steels has certain technological and economic advantages. One of these advantages is the elimination of tundish nozzle clogging in the continuous casting process: a phenomenon whereby the alumina spout, which conducts metal from the tundish to the mold, progressively plugs, restricting flow and necessitating replacement. The plugging is associated with alumina inclusions in the steel (a product of deoxidation) which sinter to the nozzle walls. In effect, therefore, the nozzle is acting as a crude melt purification process, indicating that at these high temperatures filtration is not only feasible, but will also be effective due to the rapidity of the kinetics.

On the other hand, the filtration of molten aluminum and its alloys has been a commercial reality for many years and has traditionally been associated with products such as aluminum foil. More recently, however, the increasing

use of aluminum in thin walled beverage cans, computer memory discs, demanding
aerospace applications and utilization in decorative products, such as automotive
trim, etc., has placed a renewed emphasis on melt cleanliness.

The particles present in molten metal prior to casting are an inevitable
feature of the production route and may be characterized as:

(i)   Exogeneous inclusions: these are either unavoidly present, such
        as refractory particles, or maybe inadvertently added such as
        coarse clusters of grain refiner, etc.

(ii)   Fluxes and salts suspended in the melt as the result of a prior
        metal treatment process.

(iii)   Deoxidation products as the result of a prior metal treatment process,
        e.g., Al_2O_3 (solid) or SiO_2 (liquid) deoxidation products in steel.

(iv)   Oxide of the melt which is both suspended on top of the melt and is entrapped
        within it due to tuburlence, e.g., Al_2O_3 in aluminum melts.

It has been found from industrial observation that the majority of the above
particles which are deleterious to product quality lie in the range of 1-30
microns and are dilutely suspended. Removal of these non-metallic inclusions
may be accomplished by filtration. Early advances in melt refining technology
were made by Brondyke and Hess[9] of Alcoa and Brant, Bone and Emley[10] of
British Aluminum.

Since then a number of techniques have been developed and are now well
established. In this program we have concentrated on two types of filter which
have wide scale industrial application; the deep bed filter and the ceramic foam
filter.

The deep bed filter consists of a packed bed of refractory particles
(usually tabular alumina) through which the molten metal flows. The inclusions
deposit onto the grains of the filter medium due to diffusion, direct interception,
gravity, and/or surface forces. Mechanical entrapment has been observed to be
responsible for filtration of inclusions larger than 30μm; whereas, it is believed
that surface forces are responsible for the retention of inclusions smaller than 30μm.

- 2 -

The primary mode of transport of inclusions smaller than 30µm to the grain surface of the filter medium is due to flow dynamics, while surface forces are responsible for the retention of the inclusion in the case of lower temperature systems, e.g. aluminum, while in the case of high temperature systems, e.g. steels, the inclusion sinters to the filter medium . In a depth filter the inclusions are dispersed through part or all of its volume (depth). It thus has the advantage of having a large surface area for entrapment and can trap particles much smaller than the pores of the filter bed. Industrially, therefore, a deep bed filter has an extended life and is ideally suited to continuous casting operations. At the end of its life, however, it does have the disadvantage of being slow and costly to refurbish.

The ceramic foam filter on the other hand consists of a sheet of open pore ceramic foam approximately 5cm (2 inch) thick. Typically it would have 85% volume void fraction, an average pore size of 1mm, with approximately 30 pores per linear inch. It is manufactured by impregnating an open cell polyurethane foam with a ceramic slurry. The excess slurry is squeezed out so that only the filaments of the foam remain coated. The resulting body is then dried and fired at elevated temperatures. The polyurethane foam decomposes to leave a positive ceramic replica of the original organic foam. A ceramic foam filter can be installed prior to the casting station with minimal capital expenditure and merely requires preheating before use. In contrast to deep bed filters, however, it only has a limited life, the exact value of which depends on the filter area and melt cleanliness: inclusions in the melt rapidly forming a filter cake on the surface which increases in depth and progressively restricts flow. The filter is thus good only for the single drop applications; however the foam slab is relatively inexpensive, quick to change and does not require constant heating.

The goals of the current phase of this work may therefore be itemized as follows:

- Evaluate the feasibility of filtering steels and nickel based superalloys.

- Evaluate various filter media for steel and superalloys.

- Determine, compare and contrast the fundamental bed parameters of various filters with an aim to filter optimization.

- By low temperature modeling simulate the removal of liquid inclusions by filtration.

2.   BACKGROUND

In order that a rigorous, systematic study of liquid metal filtration (both ferrous and non-ferrous) could be performed, the necessary experimental apparatus and expertise had to be developed. From the experimental viewpoint the filtration of aluminum was the least difficult of the three proposed alloy systems, hence it was the first task to be addressed. A large number of depth filtration trials were made using the aluminum-titanium diboride system. Using the experience gained from this work a steel filtration apparatus was designed, completed and commissioned.

A theoretical model was proposed and compared with the results from the first phase of this investigation. Good correlation was noted and conclusions were drawn as to the inclusion removal rate and efficiency as a function of melt flow rate. This work was extended to encompass variations in deep bed filter characteristics such as porosity, length of bed, filter area, etc. By understanding the effect of these fundamentals on inclusion capture behavior and capture kinetics it was possible to begin establishing the criteria for optimization.

To further characterize the above parameters, a low temperature model
study was performed using a calcium carbonate/hydrocarbon system, with results
which reinforced the conclusions of the aluminum/TiB$_2$ system. All this initial
work has been fully detailed in the preceeding reports (AMMRC TR-80-160 and
TR-80-49).

Since this initial work, the aluminum/titanium diboride study has been
extended to evaluate an open pore ceramic filter and a system for introducing
counter-current gas flow (an industrial practice) into the deep bed filters,
has been designed.

In the steel filtration field there has been considerable activity: in
fully characterizing the inclusions formed on deoxidation in our apparatus and
also the mathematical modeling of inclusion flow trajectory in an accelerated
flow field has been performed (using the profile of a tundish nozzle as a
reference).

Finally, a low temperature model system to simulate liquid inclusions has
been selected, a filtration apparatus has been designed and is at present in
the construction stage. The model system currently under investigation consists
of ditoluyl inclusions in water passing through a filter of spherical glass
packing.

The combined results of the above work have allowed the kinetic model to
be further refined and updated, taking into account the special conditions
encountered at the higher temperature of molten steel and superalloys. This
revised kinetic model is described in the following section.

3. PROPOSED KINETIC MODEL

The model described in the preceding reports (AMMRC TR-80-160 and
TR-80-49) quantified the important variables and parameters affecting the
inclusion removal kinetics and efficiency for comparatively low temperature
melt systems, e.g. molten aluminum, where the retention of inclusions smaller

- 5 -

than 30μ is by quasi-permanent surface associated effects. This model agreed closely with the experimental results obtained in the aluminum-titanium diboride and low-temperature model systems. The rentention of inclusions at the higher temperatures necessary for steel and superalloy filtration is by a permanent sintering mechanism, hence the kinetic model has to be slightly revised so that it will effectively describe this high temperature case. The model is, at present, still limited to the short term behavior of the filter, a situation which reflects the experimental runs. The fundamental mechanisms, however, remain largely the same throughout the majority of a filter's useful life and are described below.

When a melt containing inclusions flows past the grains of a filter medium, the inclusions should deposit on the surface of the grain if the filter is to be effective. The primary mode of transport to the grain surface for inclusions smaller than 30μ is flow dynamics, while inclusions greater than 30μ have been observed to experience mechanical entrapment.

The proposed kinetic model is based on an equation which relates the overall behavior of the filter to the microscopic entrapment mechanisms as below.

$$\left(\frac{\partial \sigma}{\partial t}\right)_Z = KC \tag{1}$$

where

σ is the volume of entrapped impurity particles per unit filter volume.

t is time

K is the kinetic parameter

C is the concentration of suspended impurity particles in the bulk liquid.

Z is the distance from the inlet of the filter.

The above expression represents the rate of change of entrapped particles per unit filter volume. The parameter K is generally found to be a function of σ and is expressed as:

$$K = K_o f(\sigma) \qquad (2)$$

where K_o is a constant whose value depends on the properties of the fluid, the size and surface morphology of both the filter medium and the inclusion. In the aluminum-titanium diboride studies and in the low temperature models the function, $f(\sigma)$, is generally found that K is a function of σ, which is the concentration of entrapped inclusions, as well as a function of the melt physical properties, melt flow rates and the shape and size of the inclusions. The functional nature of K may be expressed as (11)

$$K = K_o \left(1 - \frac{\sigma}{\sigma_m} \right) \qquad (3)$$

where K_o is the kinetic parameter coefficient and σ_m is the inclusion retention capacity of the filter bed. However, in the case of superalloy and steel melts, the inclusions sinter readily with the surface of the filter media and act as a site for further entrapment of other inclusions. Thus, it may be observed that, $f(\sigma)$, will increase with σ. Furthermore, it is reasonable to assume that electrokinetic forces do not contribute to inclusion capture since the melt is electrically conductive.

Use of the kinetic expression Equation (1), in conjunction with an inclusion mass balance over a differential filter results in a first order partial differential equation (11).

Using the appropriate boundary conditions the solution can be obtained as:

$$\frac{C}{C_i} = \frac{\exp\left[\frac{C_i}{\sigma_m} \varepsilon_i \quad \phi \ (\theta - \eta) \right]}{\exp(\phi\eta) + \exp\left[\frac{C_i}{\sigma_m} \varepsilon_i \quad \phi \quad (\theta - \eta)\right] \quad - 1} \qquad (4)$$

where the subscript i refers to the inlet condition and the dimensionless parameters are:

$$\theta = \frac{t\ U_m}{\varepsilon_i L} \quad , \text{ dimensionless time} \tag{5}$$

$$\eta = \frac{Z}{L} \ , \text{ dimensionless distance} \tag{6}$$

$$\phi = \frac{K_o L}{U_m} \ , \text{ dimensionless kinetic constant} \tag{7}$$

in the above expression, ε_i is the bed porosity, t is time, U_m is the melt approach velocity, L is the height of filter bed and Z is the distance from the filter entrance.

Equation (4) gives the concentration of inclusions in the melt as a function of time and distance along the filter. For a given value of θ, Eq. (4) describes the axial composition profile. If one is interested in the exit concentration, then η will be set to unity in Eq. (4) and the resulting expression gives the outlet inclusion concentration, C_o as a function of time.

The fundamental parameter which characterizes the performance of a depth filter is the kinetic parameter K, as given by Eq. (3). However, the value of K is a function of the magnitude of the coefficient K_o and the relative bed retention σ/σ_m (see Eq. (3)). The coefficient K_o is a function of the melt velocity through the filter, U_m, the inclusion size, d_i, the filter grain size, d_g, and the melt system. The coefficient K_o can be experimentally determined by short time experiments, whereas determination of σ_m would require experiments of long duration.

A filter having a relatively finite capacity for inclusions, will reach maximum inclusion retention capacity with extended use. On the other hand,

for a filter having a very large capacity for inclusions, progressive blockage of melt flow will occur with extended use. To determine the inclusion retention capacity factor, σ_m, melts in the order of thousands of pounds must be filtered and hence would require pilot-plant scale equipment. In this study the coefficient K_o has been experimentally determined and its dependence on melt velocity has been quantified using a low temperature model, the aluminum-titanium diboride system (see AMMRC TR-80-160 and TR-80-49) and is currently being extended to steel filtration and a low temperature model with liquid inclusions. During the initial stages of filter use when the filter bed has been exposed to only a few residence times, the inclusion retention capacity value of the filter is large compared to the entrapped inclusions, that is,

$\sigma/\sigma_M \rightarrow 0$. Under this condition, it can be shown that

$$\frac{C_i}{\sigma_m} \; \varepsilon_i \;\; \phi \;\; (\; \theta - \eta \;) \;\; \rightarrow 0. \tag{8}$$

The above enables us to simplify equation (3) to

$$\frac{C(Z)}{C_i} \;=\; \exp \;\; (\; -\phi\eta \;) \;=\; \exp \;\; (\; -\frac{K_o Z}{U_m} \;) \tag{9}$$

At the exit end of the filter, the dimensionless distance, $\eta = 1$ and the above expression reduces to

$$\frac{C_o}{C_i} \;=\; \exp \;\; (\; -\frac{K_o L}{U_m} \;) \tag{10}$$

Experiments can be designed to measure C_i, C_o, U_m and L, and thus K_o, can be calculated by the use of Equation (10). The preferred approach is one in which data from many experiments can be used collectively to determine the coefficient

K_o. Rearrangement of Equation (10) gives

$$\frac{1}{U_m} = \frac{1}{K_o L} \ln \left(\frac{C_i}{C_o} \right) \qquad (11)$$

The above suggests that if K_o is not a function of the melt velocity, U_m, then a plot of $1/U_m$ vs $\ln (C_i/C_o)$ will yield a straight line with a slope of $1/K_o L$ passing through the origin. From the slope of the graph one can calculate the coefficient K_o. However, if the assumption that K_o is independent of the melt velocity cannot be made, one may express the dependence of K_o on U_m to the first order approximation as a linear function such as

$$K_o = K_o' + K_o'' U_m \qquad (12)$$

Combining the above with Eq. (9)

$$\frac{1}{U_m} = \frac{1}{K_o' L} \ln \left(\frac{C_o}{C_i} \right) + \left(-\frac{K_o''}{K_o'} \right) \qquad (13)$$

The above suggests that a plot of $1/U_m$ vs $\ln (C_i/C_o)$ will also give a straight line with an intercept of value $(- K_o''/K_o')$ and a slope of $1/K_o' L$. Hence, the two parameters K_o' and K_o'' can be calculated from the plot of $1/U_m$ vs $\ln (C_i/C_o)$.

It can be seen from Eq. (12) that the capture kinetics are a function of two terms: the first a constant, attributable to the characteristics of the filter bed, i.e. filter media size and type, bed porosity and tortuosity, flow geometry, etc.; whilst the second is a variable which modulates the expression for flow rate.

The model may be rearranged to accommodate an experimental technique where filtered samples are taken along the length of the filter bed; that

is, inclusion concentration C, as a function of height, Z is measured.
Equation (10) can be rearranged as

$$\ln\left(\frac{C_i}{C(Z)}\right) = \frac{U_m}{K_o} Z \tag{14}$$

A plot of $\ln(C_i/C(Z))$ as a function of Z will yield a straight line with a slope of U_M/K_o and passing through the origin. In this approach one need not make the assumption on the functional dependence of K_o on the melt velocity U_m. Here, a single short-time filtration experiment will enable the determination of the kinetic parameter K_o.

Of the two experimental approaches described, it is experimentally easier to use the first method for melt systems in which only the outlet and inlet samples are monitored. However, the second approach is found to be effective in the low temperature model system studies.

4.   PROGRESS TO DATE

The phase of the work investigating the filtration of the aluminum-titanium diboride system through deep bed filters has been completed. The study has now been extended so that the performance of a ceramic foam filter may be compared. The steel filtration study has been continued; a thorough investigation of the inclusions formed during deoxidation having been undertaken and completed. Preliminary filtration runs have also been performed. In tandem with this work a mathematical model of inclusion trajectory in a converging flow field has been developed. Using experience gained from the first low temperature model study another low temperature model is currently under investigation. This work utilizes ditoluyl inclusions in water to simulate the removal of liquid inclusions from melt systems, e.g. Silica from steel melts. Each of these activities is further discussed below.

4.1 Aluminum Filtration

Using the experience gained during the deep bed filtration stage of the work the apparatus was modified, so that it would accommodate the ceramic foam filter, yet still meet the experimental requirements of: sustained heating, adequate head and metal flow rates in the range of 1 - 17 Kg/(m^{2}s) i.e. filter factors of 5 - 90 lbs./in^2 hr. The filter apparatus consisted of a graphite fixture (Figure 1), in which a two inch thick disc of the ceramic foam filter material was inserted. A refractory lined steel cylinder was cemented to the fixture to complete a filtration "module". Five of these "modules" were then placed in a special resistance furnace, so modified that molten aluminum was able to enter and exit the assemblies while they were in the furnace, precluding the freezing of the aluminum.

The size of the orifice at the bottom of the graphite fixture as well as the metallostatic head within the apparatus regulate the flowrate through each module. A steel taper placed in the orifice of each module acted as an on/off valve to control the flow of metal.

The melt to be filtered was prepared exactly as for the deep bed runs (see AMMRC TR-80-160 and TR-80-49). A filtration run consisted of pouring a transfer crucible containing approximately 25 lbs. of aluminum titanium diboride suspension into the filtration apparatus. Once the proper metallostatic head had been attained the steel taper was removed from the orifice and the filtered metal was collected in cast iron molds. Flowrates were manipulated to give filter factors in the range of 5 - 90 (lb/hr-in^2). Samples of the melt system were taken from the transfer crucible prior to filtration, and outlet samples were taken periodically from the filter apparatus. The flowrate (cm^3/s) was measured by collecting the filtrate over a specified period of time and determining its weight. For the flowrates involved in these experiments it was not difficult to maintain the required metallostatic head (approximately 18.0 in.) and it is estimated that the metallostatic head varied no more than

±10% over the course of the experiments.

In addition, an experiment was performed to determine the long term behavior of the ceramic foam filter material. An apparatus similar to that used in the previously described filtration experiments was used; the only essential difference being that a smaller filter disc was employed. In contrast with the other filtration runs, approximately 130 lb. of aluminum was passed through the foam filter disk in this experiment; while all other procedures remained the same. All inlet and outlet samples were then chemically and spectrographically analyzed for TiB_2 content. Selected inlet and outlet samples along with certain infiltrated filter discs were cut, mounted, electropolished and metallographically examined.

Although the results of this work are still to be fully analyzed, preliminary results and discussion are presented in Section 5.1.

4.2 Steel Filtration

In the preceding report (AMMRC TR-80-49) details of the steel filtration apparatus were described. An instrumented load cell attached to the receiving crucible records the accumulated melt weight instantaneously. Accurate flowrate measurements are needed to evaluate the filter coefficient, λ.

The primary motive here is to identify and quantify the kinetics of inclusion removal. Experimental determination of the kinetic parameter requires a number of filtration runs at different flow rates. Measurement of the inclusion (Al_2O_3) concentration in the inlet and filtered melt at different flowrate allows one to calculate the kinetic constant K_o (equation 2), which is a fundamental property. The filtration efficiency, η, may then be calculated.

An extensive literature survey was conducted which revealed that the refractories Al_2O_3, MgO, ZrO_2 and Cr_2O_3 are good candidates for filter material. At present Al_2O_3 filter material is being studied. To determine the effectiveness

of the filtration process, alumina inclusions were intentionally formed in the melt in the same manner as was done by Braun et. al (12). Approximately the first 20 filtration runs were made using electroytic iron as starting material. The oxygen content of this electrolytic iron was very high – approximately 1200 to 1800 ppm. Several runs were made to determine the nature of inclusions formed when cooling the melt in the furnace, or quenching on a steel plate. In runs (#21 to #27), the melt was contained in an alumina crucible. Samples from each run were sent out for expert inclusion analysis by a specialist in the field. The results show the electrolytic iron which was used in earlier experiments contained oxygen greater than 580 ppm, thus resulting in hercynite formation when aluminum was added. Addition of suitable amount of carbon reduces the initial oxygen level of the melt and further addition of aluminum then results in alumina precipitation without hercynite formation. In light of practical problems, alumina removal is far more important than hercynite removal. Hence, a 60 pound ingot containing C – 0.012%, O – 13 to 22 ppm, Ni < 0.04%, was obtained.

Using this low oxygen content iron three filtration runs were made. The oxygen level of the melt was brought up to 400 ppm by appropriate addition of Fe_2O_3. Deoxidation was carried out with 0.1% aluminum. Samples of unfiltered and filtered melt are currently being analyzed. Microscopy of cut samples from these runs show that there is a significant reduction in inclusion count in the filtered metal; however, to determine filtration efficiency, chemical analysis is needed.

The inclusion observations and discussion are presented in Section 5.2 together with some results from the preliminary scoping filtration experiments.

- 14 -

4.3 Inclusion trajectory in a converging flow geometry: A study of
the nozzle clogging phenomenon.

Singh [13] experimentally showed that the blockage of tundish nozzles by aluminum-killed steels was caused by an agglomeration of primary alumina inclusions due to aluminum deoxidation. Since inclusions are being removed during clogging of tundish nozzles, this may be fundamentally viewed as a melt purification process. To better understand the mechanism of tundish nozzle blockage and to investigate its relationship to melt purification, a mathematical model was developed by applying a force balance to an inclusion. This force balance was then integrated to obtain the trajectory of the inclusion through the tundish nozzle. The specific nozzle used in Singh's studies can be thought of as a channel having a converging geometry (see Figure 2). An understanding of the inclusion trajectory within the converging channel as well as the capture mode of the inclusion in the channel is complementary to the kinetic model which deals with the kinetics of inclusion capture in filters.

A computer program was written to use the Runga Kutta method of integration to find inclusion trajectories for various initial positions in the nozzle. The trajectory which terminates exactly at the end of the nozzle wall is called the limiting trajectory (see Figure 3). All trajectories to the wall side of the limiting trajectory contact the nozzle and result in inclusion collection. In contrast, trajectories lying on the other side of the limiting trajectory (i.e., towards the nozzle center) pass through unimpeded. Thus, knowledge of the limiting trajectory allows one to calcualte the fraction of inclusions which contact the nozzle wall - the collection efficiency.

The effect of the different terms in the force balance equation (force balance applied to an inclusion moving through the nozzle) on collection efficiency was evaluated. The steady state drag force balance is:

$$m \frac{du}{dt} = (m_\ell - m) g - \frac{\pi}{2} C_d R_p^2 \rho_\ell U|U| \tag{15}$$

- 15 -

Equation (15) is termed the steady state drag force balance because it applies to an inclusion moving at steady state (not being accelerated) an infinite distance away from any solid boundaries. In equation (15) M is the mass of the inclusion. U is the inclusion velocity relative to the fluid, t is time, m_ℓ is the fluid mass displaced by the inclusion, g is the acceleration of gravity, C_D is the drag force coefficient, R_p is the inclusion radius, and ρ_ℓ is the fluid density. A collection efficiency of 1.71% was found by using equation (15) and utilizing industrial operating condition values.

Subsequently, the increase in drag force due to inclusion motion close to a solid boundary was considered. Inclusion motion towards the nozzle wall is impeded by the added energy required to drain fluid out from between the inclusion and the nozzle wall. The force balance equation, which takes into account this drainage effect is

$$m \frac{dU}{dt} = (m_\ell - m)g - \frac{(\pi/2) C_D R_p^2 \rho_\ell U|U|}{1 - \frac{k R_p}{\ell}} \tag{16}$$

where the constant k is a function of geometry and ℓ is the distance of the inclusion from the nozzle wall. Using equation (16) a collection efficiency of 1.65% was obtained. This is less than the efficiency found previously (equation 15) because the acceleration on an inclusion towards the nozzle center is increased as it approaches the nozzle wall.

To take into consideration the effect of acceleration on the trajectory of an inclusion, two additional terms are considered and subsequently included in the force balance. The first term to be included is the added mass term, which accounts for the acceleration of the fluid adjacent to the inclusion. The force balance then becomes

$$m \frac{dU}{dt} = (m_\ell - m)g - \frac{(\pi/2) C_D R_p^2 \rho_\ell U|U|}{1 - \frac{k R_p}{\ell}} - C_A m_\ell \frac{dU}{dt} \tag{17}$$

where C_A is the added mass coefficient. When this equation was used in the computer program it was found that 2.9% of the inclusions passing through the tundish nozzle are collected. This is an increase over the previous cases because the added mass term decreases the inclusion's acceleration towards the nozzle center.

The second term to be added to the force balance equation is the history term which takes into account the dependence of the instantaneous drag force on the state of development of the boundary layer around the inclusion. In this case, the force balance equation is

$$m \frac{dU}{dt} = (m_\ell - m)g - \frac{(\pi/2) \frac{C_D R_p^2 \rho_\ell U|U|}{k R}}{1 - \frac{p}{\ell}} - C_A m_\ell \cdot \frac{dU}{dt} \qquad (18)$$

$$- C_H R_p^2 \left(\pi \rho_\ell \mu\right)^{1/2} \int_0^t \frac{dU}{d\tau} \cdot \frac{d\tau}{\sqrt{t-\tau}}$$

where C_H is the history coefficient and τ is a dummy variable of integration. By the use of eq. (18), a 5.2% collection efficiency is obtained. This is larger than the collection efficiency found in all the preceding cases since the history term increases the inclusion acceleration towards the nozzle wall.

The above proposed model is compared with the experimental results obtained by Singh (13) in Section 5.3.

4.4 <u>Low Temperature Model System to Simulate the Filtration of Liquid Inclusions</u>

To simulate the removal of liquid inclusions from melt systems e.g., SiO_2 in steel or halide salts (a product of reactive gas "cleaning") in aluminum, a low temperature model system consisting of an emulsion of 0.01% 3-3 dimethyl-diphenyl in distilled water has been developed. The emulsion has the following unique properties: (i) the suspension is very stable over several days with

liquid inclusions in a narrow size range of 2 to 4μm; (ii) the density

difference between water and ditoulyl is essentially zero thus enabling

the determination of kinetics of filtration free of settling effects:

(iii) the difference in refractive index between water and ditoulyl is high,

thus enabling easy visualization.

An apparatus to study filtration in this system is currently under

construction. It will consist of five evenly spaced beds of glass beads

each of 5cm height, contained within a 6.3cm diameter plexiglas column.

Sample ports will be placed at the inlet and after each bed.

It is envisaged that an experimental run will proceed as follows: first,

the model melt system will be prepared. This will be an emulsion of 0.01%

3-3 dimethyl-diphnyl in distilled water which will be left overnight to

stabilize droplet size. Scoping experiments with this emulsion have shown

that the droplets range from 2 to 5μ; as 3-3 dimethyl-diphenyl has a density.

similar to water, the emulsion formed is stable for several days without the

addition of surfactants. The emulsion will be pumped upwards through the

column and samples will be taken between every 1-2 residence time periods until

the filter appears to be saturated. The samples will then be immediately diluted

with an equal weight of ethanol , in which both of the emulsion components are

soluble. This will allow for spectrophotometric analysis of 3-3 dimelthyl-

diphenyl concentration, although some further dilution may be necessary to bring

the solution into the absorbance range (0-9 p.p.m for ditoulyl) of the spectro-

photometer.

There are three variables in the experiment: velocity,grain size and inter-

facial tension. It is proposed to vary the velocity between 0.015 cm (A range

of industrial interest) for a combination of grain size (glass bead size) and inter-

facial tension. Flow and logistic considerations would dictate glass beads of 3mm

and 5mm diameter, while their interfacial tension can be varied by baking a film

of silicone oil onto the surface. This changes the glass surface from one not

wetted by the diphenyl, to one which is partially wetted.

5.   RESULTS AND DISCUSSION

5.1   Aluminum filtration: The ceramic foam filter

The results of the filtration experiments are presented in Table 1
and graphically represented in figures 4 to 10.   Figure 4 shows the
filtration efficiency is represented by η, where η is the function of
inclusions removed, i.e.

$$\eta = \frac{C_i - C_o}{C_i} \tag{19}$$

As can be seen from the figure at low melt velocities the efficiency
of titanium diboride inclusion removal approaches 100%, while at higher
velocities (greater than 0.5 cm/sec), the efficiency of inclusion removal
levels off to a value between 40% and 60%.

Figure 5 shows a plot of $\ln(C_i/C_o)$ vs $1/U_m$, which as predicted by
the proposed kinetic model, is of a linear nature.   It may also be seen
that the line clearly does not intercept the origin, hence the filter
behavior will fall into the regime where the kinetic parameter, K_o, is
a function of the melt approach velocity, U_m.   Figure 6 shows the de-
pendence of K_o on the melt velocity, where it can be seen that the func-
tionality may be analyzed by use of equation (12).   Analysis of the K_o
function yields $K_o = 0.018 + 0.062\ U_m$, the first term being the value
of the intercept and hence reflects the intrinsic characteristics of the
filter, whereas the second term is the slope and is related to the flow
rate dependency of the filter.

Figure 7 shows the filtration coefficient, λ, (see AMMRC TR-80-160
and TR-80-49) as a function of melt velocity.   It can be seen that the
value of λ initially drops rapidly with increasing velocity, levelling

off, however, after about 0.40 cm/sec. This would indicate that to maintain good filter performance the melt velocity has to be low, or if production constraints necessitate a higher velocity, then a longer filter length would be required. This information is reinterpreted in figure 8 which shows the relationship of Λ to melt velocity. It can be seen that Λ, the depth of filter required to remove 63% of the incoming inclusions (see AMMRC TR-80-16 and TR-80-49), increases with increasing melt velocity.

As outlined in the introduction, the longer term behavior of a ceramic foam filter is expected to be substantially different to that observed in the short term. This disparity in behaviors would be expected due to the rapid build up of a filter "cake" on the top surface of the foam. An experiment to monitor this cake formation was performed. The superficial melt velocity was measured as a function of time, the results are presented in Figure 9. It can be seen that the melt approach velocity, U_m, initially remained fairly constant, then abruptly dropping and leveling off to a value much lower than the initial melt approach velocity. A plot of $\Delta t/\Delta V$ as a function of $\overline{V}$, Figure 10, where ΔV is the increment of filtrate collected over a time period Δt, and $\overline{V}$ which is $(V_1 + V_2)/2$ of each increment of filtrate volume, indicates that the ceramic foam filter in this run exhibits behavior characteristic of a cake filter where $dt/dV = (K_1/P)\overline{V} + (K_2/P)$ for constant pressure cake filtration, i.e., where the metallostatic head remains constant; (K_1/P), (K_2/P) constants for a particular filtration system. A plot of the cumulative filtrate volume, i.e., the total volume of aluminum melt passed through the apparatus, as a function of time indicates that the 1.0" diameter

ceramic foam filter disk used in the long term filtration run progressed from an initial packed bed mode of filtration, where the flow rate remains essentially constant, to a cake filtration mode, after approximately 8500 cm^3 of aluminum had passed through the system. This analysis is based on the fact that as the cake forms and builds up, the pressure (ΔP) required to force metal through the cake increases; however, since this was a constant pressure operation where $\Delta P = \rho g h$, h being the metallostatic head, the driving force decreases, resulting in a steadily decreasing flow of metal through the system, which was in fact observed.

Subsequent metallographic examination of the filter disk used in the long term filtration run clearly showed that a cake had formed on the top surface. Although inlet and outlet samples were taken during this run they cannot be used to estimate σ_m, the available capture volume of the filter because: (i) the filter enters a cake filtration mode which is not encompassed by the proposed kinetic model; (ii) the samples are analyzed only for titanium diboride content, hence there is no information as to the total volume and number of inclusions present in the melt.

It should also be noted that the results obtained from spectrophotometric analysis provide only quantitative information about the titanium diboride content; they give no indication of a qualitative nature, i.e. the effect of filtration on inclusion size distribution is unknown. It is believed that inclusion particle size is an important factor in determining filter performance, however particle size analysis is a slow, costly and specialized procedure; hence the effect of this variable in all the experiments has been minimized by using a con-

sistent titanium diboride master alloy, systematic stirring, etc.

5.2 Steel Filtration

To date 31 filtration runs have been made. Many of those were scoping experiments to debug the apparatus and to verify the nature of the deoxidation products which were being "manufactured". The inclusion observations are summarized in Table 2. In some runs Fe-10% Ni alloy was used as the starting material, rather than pure iron. The purpose of this was to assist in etching the structure, hence better delineating the portion of the inclusions in relation to the solidification structure. Table 3 summarizes the successful filtration experiments. In both runs numbers 5 and 10 the Al_2O_3 was reduced approximately seven-fold (from 0.0784 to 0.0116 and 0.1945 to 0.0264, respectively), whereas the total oxygen was reduced between 2 to 4 times.

It is expected that as the apparatus has now been debugged and standardized, filtration runs will proceed apace, resulting in the following contributions:

    (i)   The major mechanism by which particles are entrapped in the filter medium will be identified.

    (ii)   The functional nature of the particle capture kinetics in steel melts will be developed.

    (iii)   The kinetic parameter, K_o, and the filtration coefficient, λ, will be experimentally determined.

    (iv)   The effect of the important operating (process) variables on the performance characteristics of the filters will be determined.

5.3 Inclusion Trajectory in a Converging Flow Geometry

The proposed model may be compared to Singh's[12] experimental results. Singh reported that flow through the nozzle shown in Figure 2 became greatly reduced after 21 minutes. The inclusion trajectory model proposed here predicts that at Singh's casting conditions, 1.5% of the inclusions passing through the nozzle will be collected. THis value of 1.5% collection gives a total volume of collected inclusions of 21 cm^3 which is more than enough to reduce the flow through Singh's nozzle. The bottom section of Singh's nozzle has a volume of approximately 40 cm^3. Since alumina inclusions readily sinter together there is a great deal of void space in the bulk agglomerated alumina at the nozzle exit. Thus, the total volume of the agglomeration is much more than 21 cm^3 and the inclusion trajectory model successfully explains the tundish nozzle blockage phenomenon.

The important result of this phase of the program is the similarity of the mechanism of nozzle blockage to the inertial impaction mechanism of impurity removal in depth filtration[14]. This indicates the high potential of depth filtration as a viable process for melt purification.

6. FUTURE WORK

Work is planned in several different areas:

6.1 Aluminum Filtration

- The performance of the deep bed and ceramic foam filters will
  be compared and contrasted with reference to the kinetic model.

- The industrial practice of passing counter current gas flow
  through a deep bed filter will be evaluated.

- A series of filtration experiments will be conducted using a
  ceramic filter, the tortuosity and surface area of which are
  readily definable.

6.2 Steel Filtration

- The efficiency of filtration will be evaluated initially using
  Al_2O_3 tabular beds.

6.3 Superalloy Filtration

- Evaluation of filtration efficiency initially using Al_2O_3 tabular
  beds. Work is currently in progress to design modifications to
  the steel filtration apparatus for superalloy work.

6.4 Low Temperature Modeling

- The current work extending the original diesel/calcium carbonate,
  solid inclusions system, to the liquid inclusion system will be
  continued. It is expected that the model will elucidate the
  effect of factors such as velocity, grain size and interfacial
  tension on the performance of a filter removing liquid inclusions.

- This work may be extended to include a flow visualization study
  which will pictorially record and illustrate the capture, satura-
  tion and subsequent release phenomena of liquid inclusion in
  packed beds.

REFERENCES

1. F.R. Mollard, N. Davidson, "Ceramic Foam - A unique Method of
    Filtering Molten Aluminum in the Foundry", presented at the 1978
    AFS Conference, Detroit, Michigan.

2. R.B. Miclot, Technical Report No. 67-1507, Rock Island Arsenal,
    June 1967.

3. L.A. Alekseev, I.B. Kumanin, Izv. Vyssh. Uchebr. Zaved. Tseutn.
    Metall., Vol. 11, No.1 (1968), pp. 155-159.

4. D. Apelian, ScD. Thesis, MIT, 1972.

5. H.E. Miller, Aluminum (1972), pp. 368-371.

6. Dj. Hedjazi, G.H.J. Bennett, V. Kondic, Metals Technology, Dec.
    (1976) pp. 537-541.

7. A.I. Kemppinen, G.D. Schnittgrund, Light Metals, Vol. 2 (1969),
    pp. 721-732.

8. J.J. Farber, F.M. Rupp, Light Metals, Vol. 2 (1979), pp. 733-740.

9. K.J. Brondyke, P.D. Hess, Trans. TMS-AIME (1964), Vol. 230, pp.
    1553-1556.

10. M.V. Brant, D.C. Bone and E.F. Emley, Journal of Metals, March (1971)
    Vol. 23, pp. 48-53.

11. D. Apelian, R. Mutharasan, "Filtration, a Melt Refining Method",
    Journal of Metals, September (1980), Vol. 32, No. 9, pp. 14-19.

12. T.B. Braun, J.F. Elliot, and M.C. Flemings: Met. Trans. Vol. 10B,
    June 1979, pp. 171-184.

13. S.N. Singh: I & SM Journal, June 1979, pp. 40-46.

14. L.A. Spielman: Ann. Rev. Fluid Mech., 9:297, 1977.

TABLE 1

Summary of Filtration Results

Sample	U_m(cm/s)	$1/U_m$	C_i(ppm)	C_o(ppm)	$n=\dfrac{C_i-C_o}{C_i}$
ST201	0.22	4.53	979.2	382.5	0.61
ST202	0.22	4.53	979.2	489.6	0.50
ST301	0.153	6.54	750.0	351.9	0.53
ST302	0.153	6.54	750.0	183.6	0.76
ST401	0.075	13.32	1040.0	168.0	0.84
ST501	0.056	17.92	581.4	137.7	0.76
ST603	0.451	2.22	45.2	22.9	0.49
ST701	0.775	1.29	26.8	16.8	0.37

TABLE 2

Observation of Inclusion in Different Experiments

Run Number	Charge	Experiment	Observations
21	Electrolytic iron & Fe_2O_3 in alumina crucible in argon atmosphere.	Melted at 1600°C, melt is held for 30 min. at 1600°C, solid aluminum (0.09 wt%) is dropped in the melt. The induction power was shut off after 5 min. of aluminum addition.	Duplex inclusion SEM study shows the presence of Fe, Al and O in inclusions. Size of inclusion: 2–40µm. Near crucible wall clusters of inclusions were present.
22	Electrolytic iron melted at 1600°C in alumina crucible in argon atmosphere.	No Al or Fe_2O_3 was added. The sample was held as 1600°C for 1 1/2 hrs, and then furnace cooled.	Spherical inclusions of size 2–10 µm were present. SEM study shows the presence of Fe and O in inclusions.
27	Electrolytic iron + 0.025 % C in alumina crucible in argon atmosphere.	Melted in vacuum ($\sim$ 10 microns) and then furnace cooled after holding at 1600°C for 30 min.	The sample was very clean. Negligible amount of small inclusions 1 to 5 µm were present.

TABLE 3

Summary of Filtration Experiments

Run No.	Wt % Al$_2$O$_3$		Wt % Oxygen	
	Inlet to filter	Outlet	Inlet to filter	Outlet
5	0.0784	0.0116	0.0365	0.0114
8	0.2644	0.0019	0.1800	0.1000
10	0.1945	0.0264	0.1700	0.0600
20	0.1210	0.0180	0.0914	0.0203
28				
29				
30	analysis unavailable at the time of writing this report			
31				
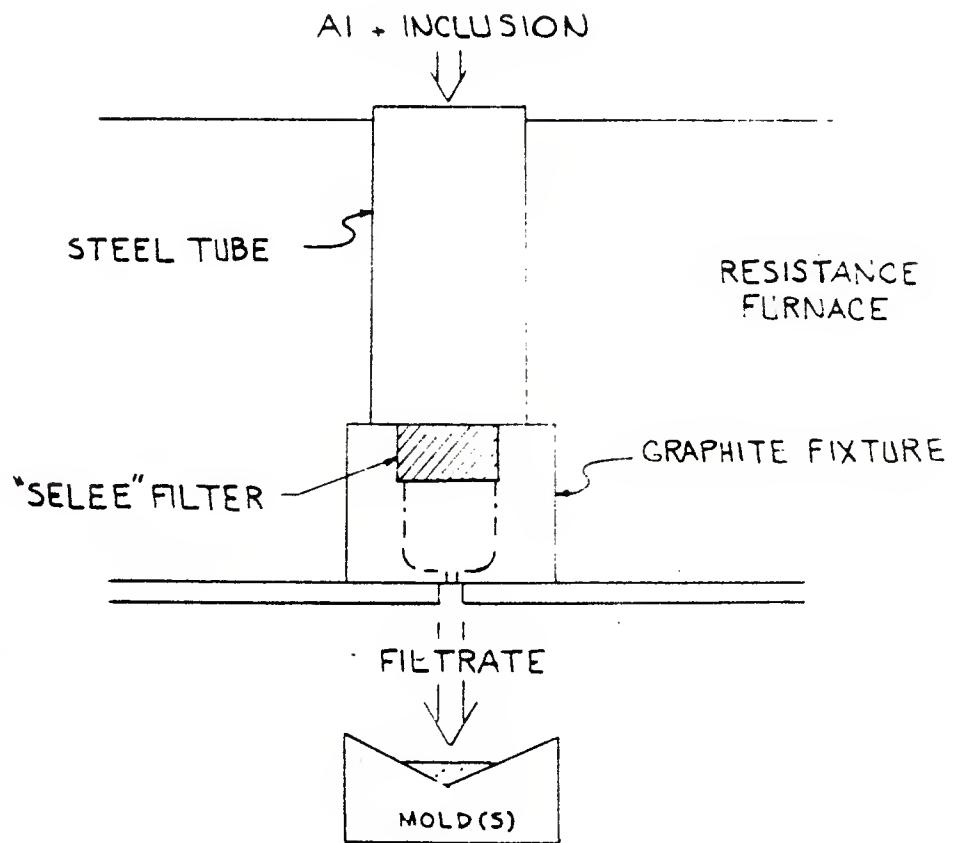
Figure 1. A schematic of the Ceramic Foam Filtration Apparatus used in the investigation of short-term filter behavior.
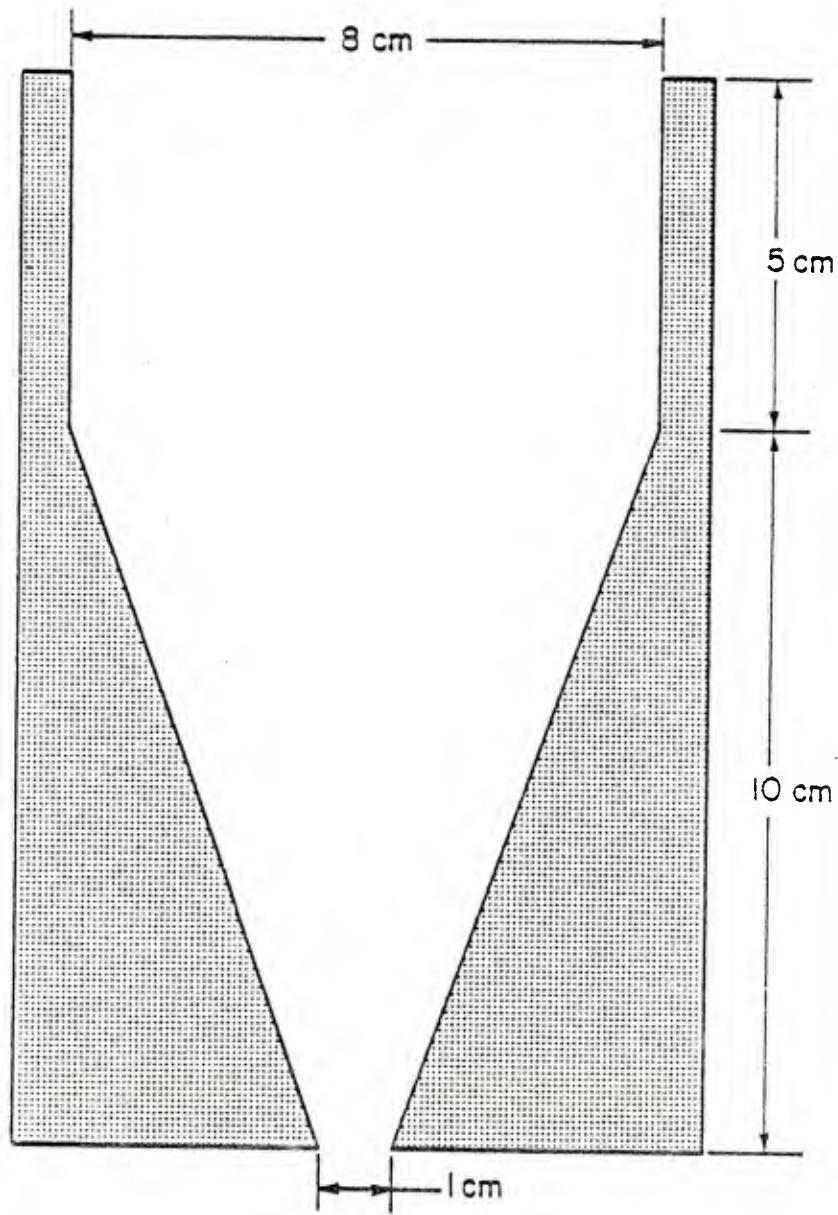
Figure 2. Schematic diagram showing dimensions of the converging nozzle geometry studied by Singh[13].
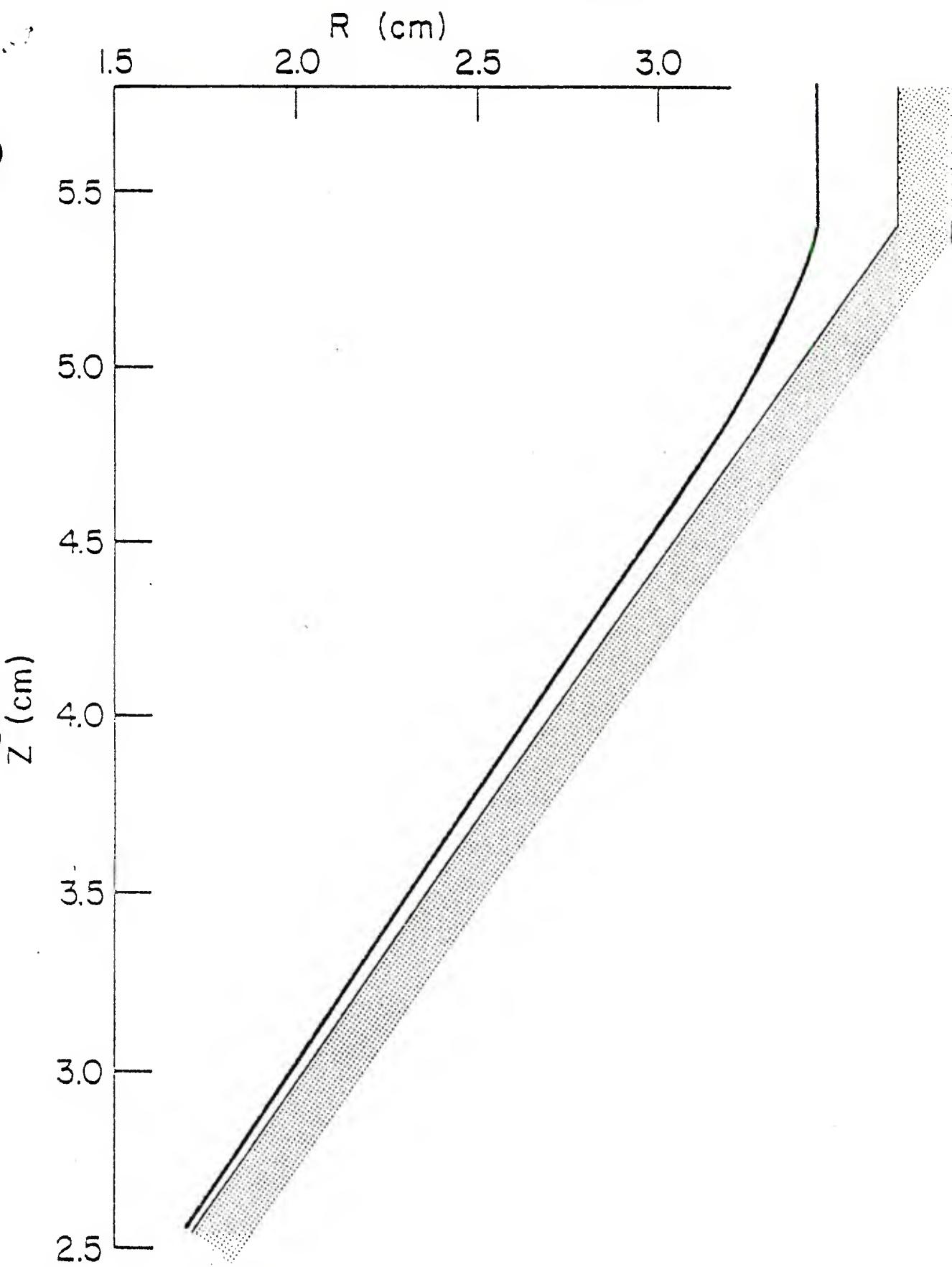
Figure 3. Limiting trajectory computed from the model (equation 9) shown at the exit side of the converging nozzle. Z indicates the height from the nozzle exit, and R is the radial distance from the nozzle center.
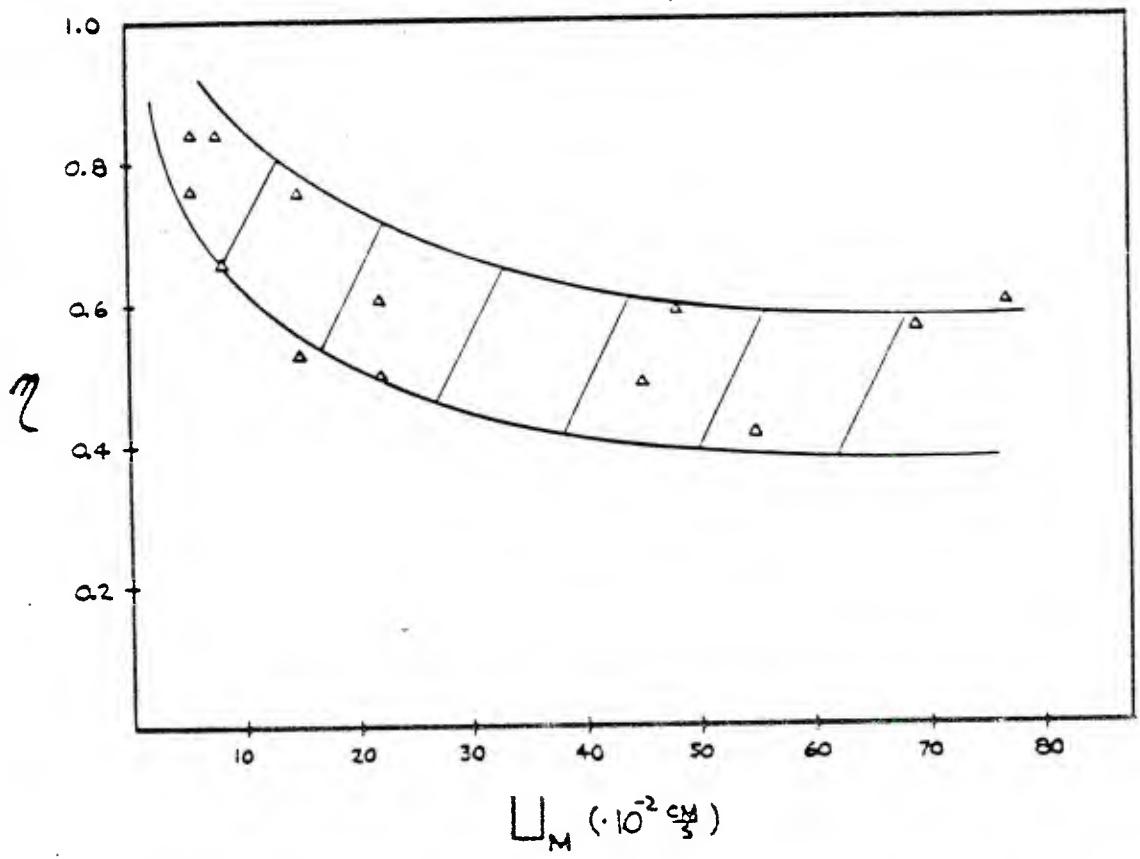
Figure 4. TiB$_2$ inclusion removal efficeincy, $\eta = \dfrac{C_i - C_o}{C_i}$, as a function of the melt approach velocity, U_m.
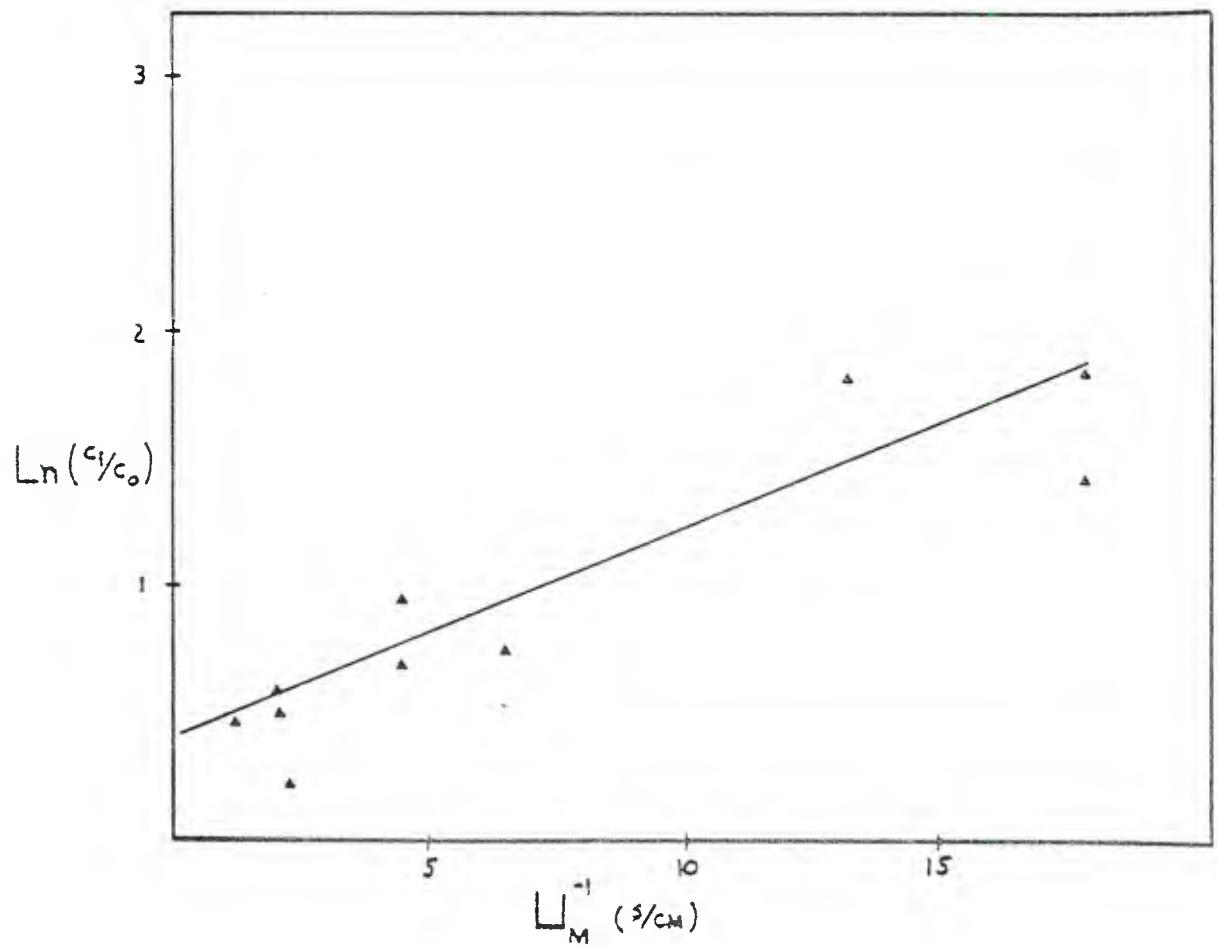
Figure 5. $\ln \dfrac{C_i}{C_o}$ as a function of the reciprocal of the melt approach velocity, U_m.
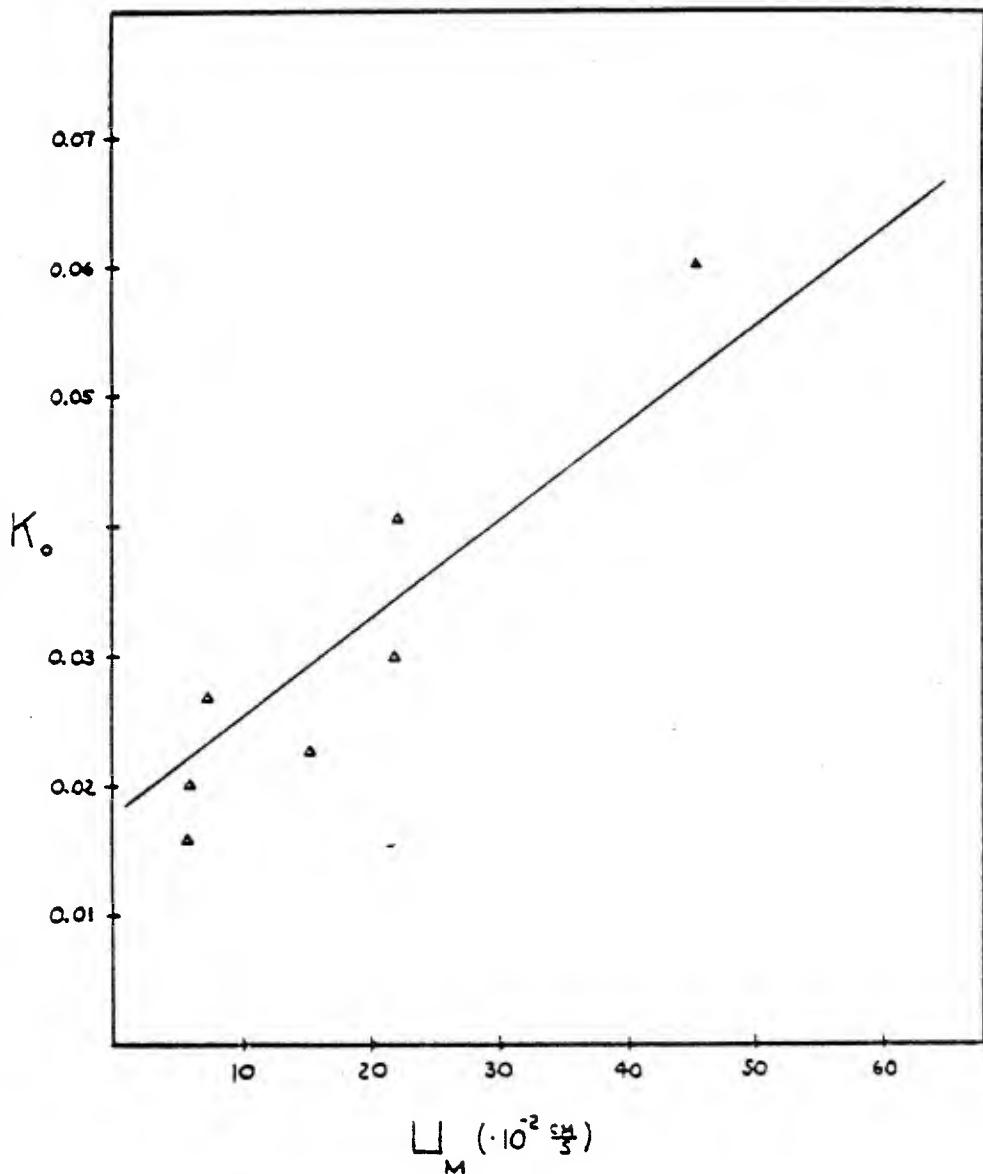
Figure 6.   Kinetic parameter, K_o, as a function of the melt approach velocity, U_m.
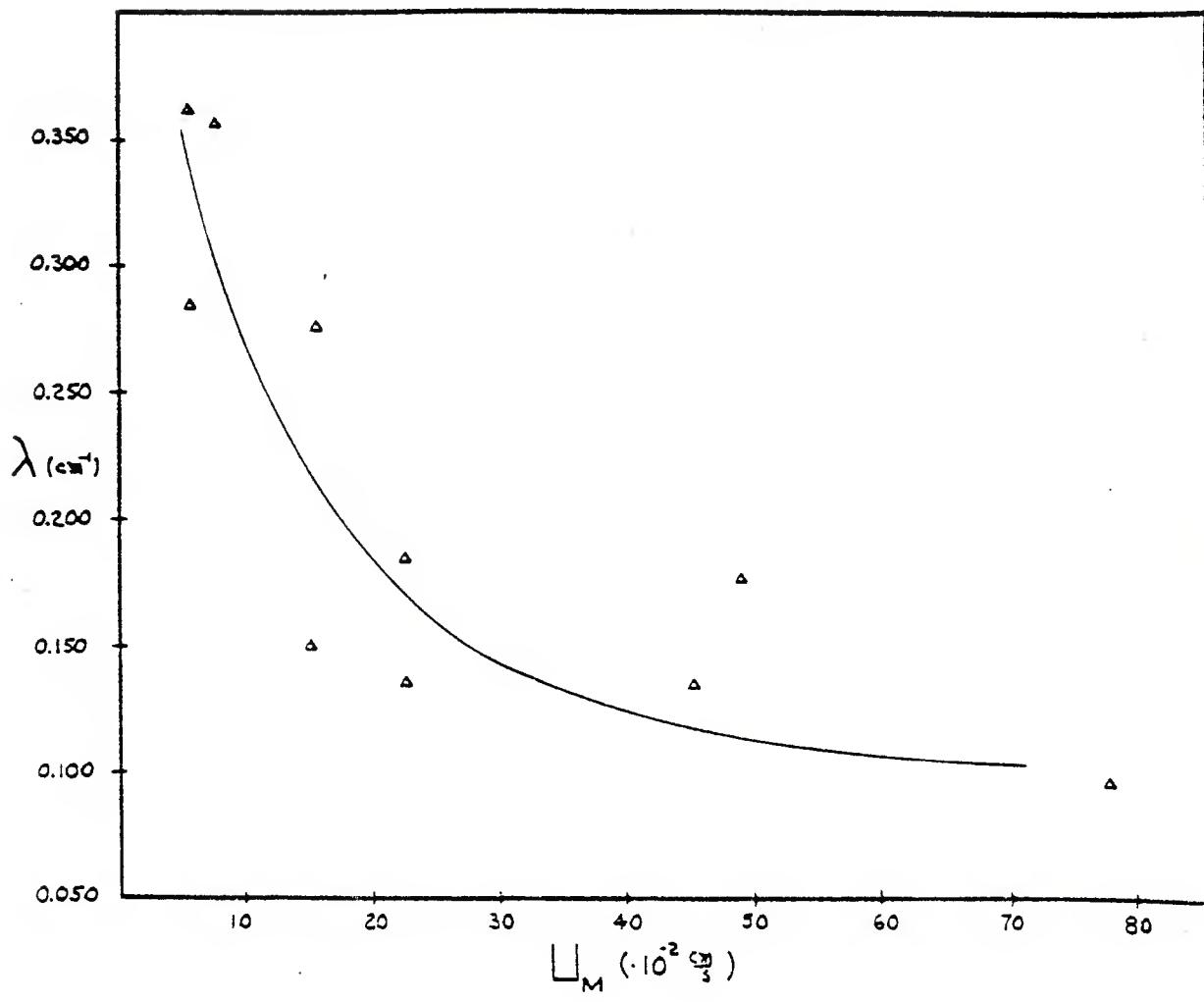
Figure 7. λ, i.e. $\dfrac{K_o}{U_m}$, as a function of the melt approach velocity, U_m.
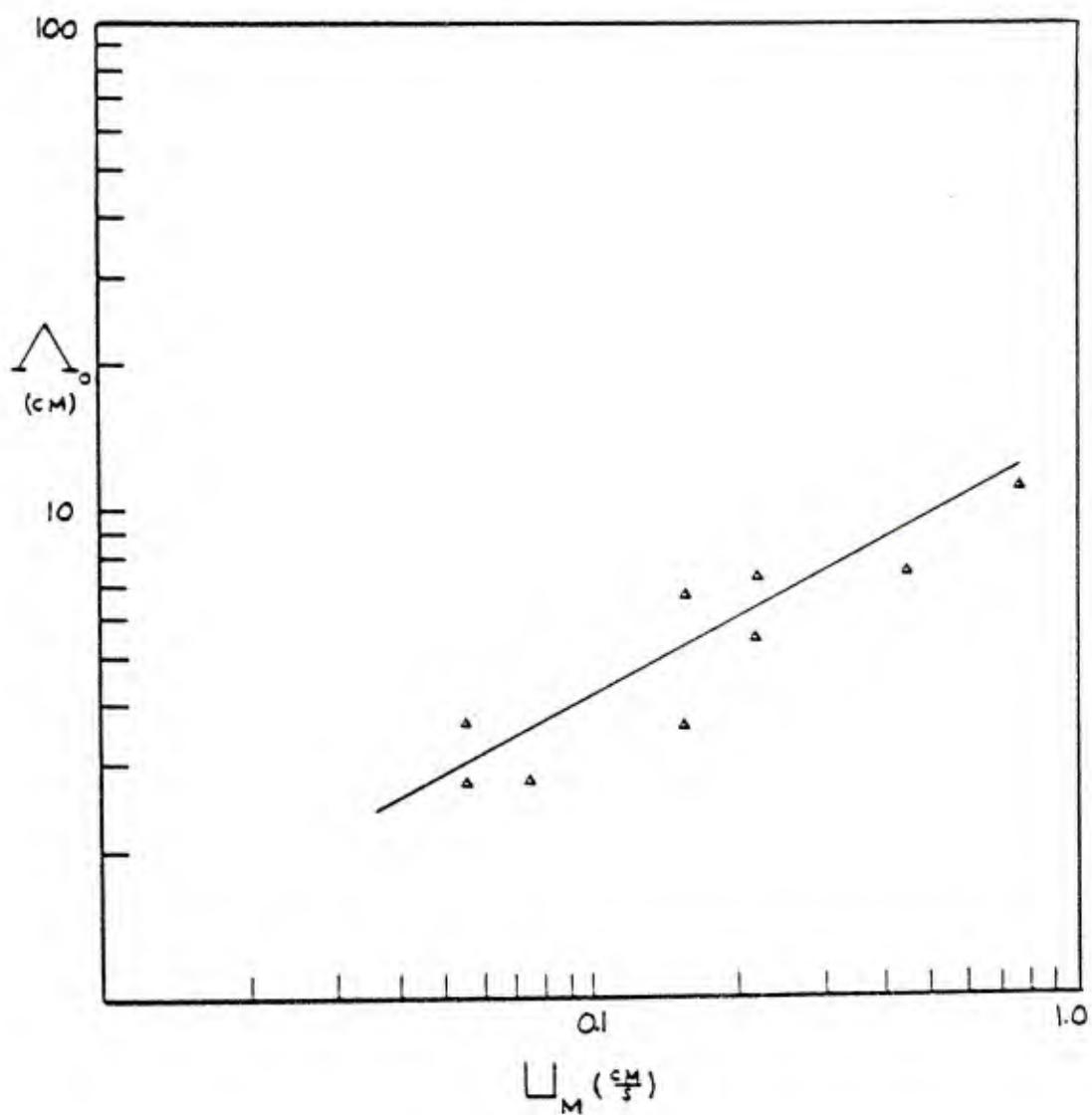
Figure 8. Depth of ceramic foam required to remove 63% of TiB_2 inclusions, Λ, as a function of the melt approach velocity, U_m.
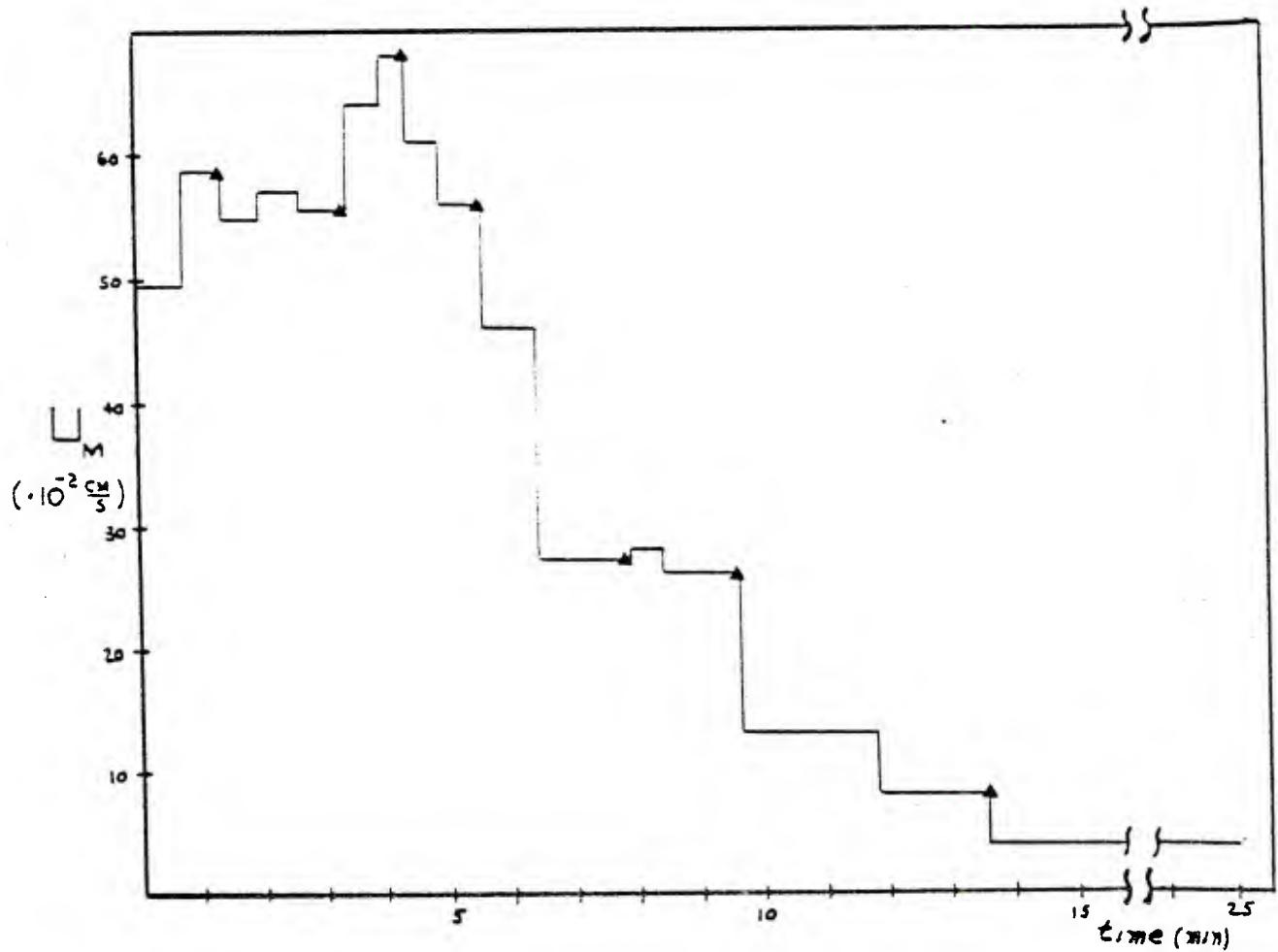
Figure 9. Melt approach velocity, U_m, as a function of time for the long term filtration experiment. ▲ denotes the time at which an outlet sample was taken.
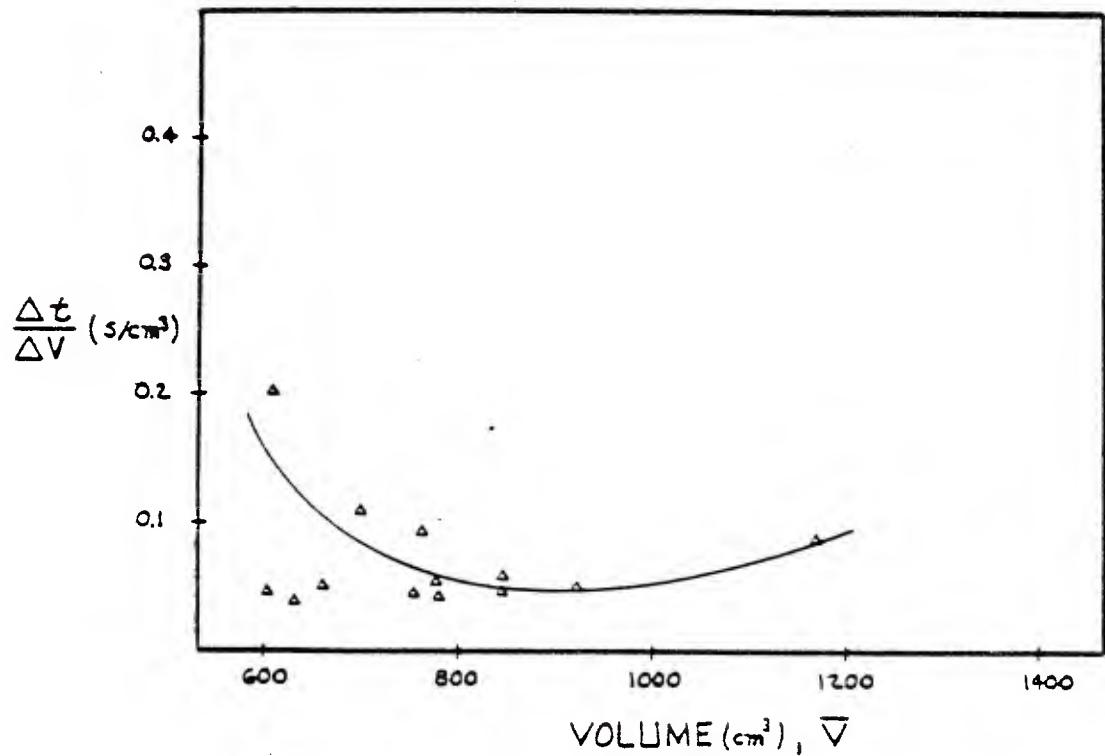
Figure 10. The reciprocal of the increment of filtrate volume collected over a period of time, $\Delta V / \Delta t$, as a function of $\overline{V}$, which is $(V_1 + V_2)/2$ of each increment of filtrate volume.

No. of Copies	To
1	Office of the Under Secretary of Defense for Research and Engineering, The Pentagon, Washington, D.C. 20301
12	Commander, Defense Technical Information Center, Cameron Station, Building 5, 5010 Duke Street, Alexandria, Virginia 22314
1	Director, Defense Advanced Research Projects Agency, 1400 Wilson Boulevard, Arlington, Virginia · 22209

Metals and Ceramics Information Center, Battelle Columbus Laboratories, 505 King Avenue, Columbus, Ohio   43201

2	ATTN: Mr. Daniel Maykuth

Deputy Chief of Staff for Research, Development, and Acquisition, Headquarters, Department of the Army, Washington, D.C.   20310

2	ATTN: DAMA-ARZ
1	Dr. Bernard R. Stein

Commander, U.S. Army Material Development and Readiness Command, 5001 Eisenhower Avenue, Alexandria, Virginia   22333

1	ATTN: DRCDE-DE, Development Division
1	DRCDE-RS, Research Division
1	DRCDE-RS, Scientific Deputy
1	DRCLDC

Commander, U.S. Army Aviation Research and Development Command, 4300 Goodfellow Boulevard, St. Louis, Missouri   63120

1	ATTN: DRDAV-LEP, Mr. J. M. Thorp
1	DRDAV-ER, Dr. I. Peterson

Commander, U.S. Army Missile Command, Redstone Arsenal, Alabama   35809

| 1	ATTN: DRSMI-IE, Mr. J. E. Kirshtein
1	DRSMI-R, Mr. John L. McDaniel
1	DRSMI-TB, Redstone Scientific Information Center
1	Chief Scientist, Dr. W. W. Carter
1	Directorate of R&D
1	Dr. B. Steverding

Commander, U.S. Army Troop Support and Aviation Materiel Readiness Command, 4300 Goodfellow Boulevard, St. Louis, Missouri   63120

1	ATTN: DRSTS, Mr. J. Murphy

Commander, U.S. Army Armament Research and Development Command, Dover, New Jersey   07801

1	ATTN: DRDAR-SCM, J. D. Corrie
2	Technical Library
1	Mr. Harry E. Pebly, Jr., PLASTEC, Director

Commander, U.S. Army Tank-Automotive Research and Development Command, Warren, Michigan 48090
1 ATTN: DRDTA-PPS, Mr. David Siegel
1   DRDTA-RCM.1, Mr. Edward Moritz
1   DRDTA-RCM.1, Mr. Donald Phelps

Commander, Aberdeen Proving Ground, Maryland 21005
1 ATTN: Technical Library, Building 313

Commander, U.S. Army Foreign Science and Technology Center, 220 7th Street, N.E., Charlottesville, Virginia 22901
1 ATTN: DRXST-MT1

Commander, Rock Island Arsenal, Rock Island, Illinois 61299
1 ATTN: SARRI-LEP-L

Director, Eustis Directorate, U.S. Army Air Mobility Research and Development Laboratory, Fort Eustis, Virginia 23604
1 ATTN: Mr. J. Robinson, DAVDL-E-MOS (AVRADCOM)

Director, U.S. Army Ballistic Research Laboratories, Aberdeen Proving Ground, Maryland 21005
1 ATTN: Dr. D. Eichelberger
1   DRDAR-TSB-S (STINFO)

Director, U.S. Army Materiel System Analysis Activity, Aberdeen Proving Ground, Maryland 21005
1 ATTN: DRXSY-MP, H. Cohen

Commander, U.S. Army Electronics Research and Development Command, 225 South 18th Street, Philadelphia, Pennsylvania 19103
1 ATTN: DRSEL-PP/P/IED-2, Mr. Wesley Karg

Commander, U.S. Army Mobility Equipment Research and Development Command, Fort Belvoir, Virginia 22060
2 ATTN: Technical Documents Center, Building 315

Commander, U.S. Army Production Equipment Agency, Manufacturing Technology Branch, Rock Island Arsenal, Illinois 61299
1 ATTN: Library

Commander, Watervliet Arsenal, Watervliet, New York 12189
1 ATTN: DRDAR-R
1   Dr. Robert Weigle (ARRCOM)

1 Chief, Bureau of Naval Weapons, Department of the Navy, Room 2225, Munitions Building, Washington, D.C. 20390

Chief, Bureau of Ships, Department of the Navy, Washington, D.C. 20315
1 ATTN: Code 341

Chief of Naval Research, Arlington, Virginia 22217
1   ATTN: Code 471

Naval Research Laboratory, Washington, D.C. 20375
2   ATTN: Dr. G. R. Yoder, Code 6384

Headquarters, USAF/RDPI, The Pentagon, Washington, D.C. 20330
1   ATTN: Major Donald Sponberg

Commander, U.S. Air Force Wright Aeronautical Laboratories, Wright-
Patterson Air Force Base, Ohio 45433
1   ATTN: AFWAL/MLTB, Mr. George Glenn
1   AFWAL/MLSE, E. Morrissey
1   AFWAL/MLLP, D. M. Forney, Jr.
1   AFWAL/MLC
1   AFWAL/MLBC, Mr. Stanley Schulman

National Aeronautics and Space Administration, Washington, D.C. 20546
1   ATTN: AFSS-AD, Office of Scientific and Technical Information
1   Mr. B. G. Achhammer
1   Mr. G. C. Deutsch, Code RW

National Aeronautics and Space Administration, Lewis Research Center,
21000 Brookpark Road, Cleveland, Ohio 44135
1   ATTN: Library

National Aeronautics and Space Administration, Marshall Space Flight Center,
Huntsville, Alabama 35812
1   ATTN: R. J. Schwinghamer, EH01, Dir., M&P Lab
1   Mr. W. A. Wilson, EH41, Bldg. 4612

Albany Metallurgy Research Center, Albany, Oregon 97321
1   ATTN: Mr. A. H. Roberson, Research Director

Defense Materials Service, General Services Administration,
Washington, D.C. 20405
1   ATTN: Mr. Clarence A. Fredell, Director, Technical R&D Staff

General Dynamics, Convair Aerospace Division, P.O. Box 748,
Fort Worth, Texas 76101
1   ATTN: Mfg. Engineering Technical Library

Cabot Corporation, Machinery Division, P.O. Box 1101, Pampa, Texas 79065
1   ATTN: W. L. Hallerberg, Director of Metallurgy

Director, Army Materials and Mechanics Research Center,
Watertown, Massachusetts 02172
2   ATTN: DRXMR-PL
1   DRXMR-PR
1   DRXMR-PD
1   DRXMR-AP
5   DRXMR-ER, Mr. A. Ayvazian

AD _____ Unclassified
Unlimited Distribution

Army Materials and Mechanics Research Center
Watertown, Massachusetts 02172
MELT PURIFICATION VIA FILTRATION
D. Apelian, R. Mutharasan and C. Romanowski
College of Engineering
Drexel University
Philadelphia, Pennsylvania 19104
Technical Report AMMRC-TR 81-29, June 1981,
42 pp.-illus.-tables, Contract DAAG46-79-C-0052
D/A Project: 1L162105AH84; AMCMS Code: 612105.H840011
Interim Report, January 1981-April 1981

Key Words

Filtration
Liquid metals
Aluminum
Steel
Superalloys
Purification

Background on the mechanisms and kinetics of filtration is discussed and the Drexel mathematical model is further elaborated and updated to encompass filtration at the higher temperatures encountered in steels and superalloys. A novel mathematical analysis of inclusion trajectory is also presented. A low temperature model The aluminum-TiB2 study has been extended to evaluate a ceramic foam filter. A low temperature model study of liquid inclusion filtration is described and discussed.
Reference is made to ongoing work in superalloy and steel filtration, counter-current gas filtration, filter characterization and flow visualization.

AD ———————————

Army Materials and Mechanics Research Center
Watertown, Massachusetts 02172
MELT PURIFICATION VIA FILTRATION
D. Apelian, R. Mutharasan and C. Romanowski
College of Engineering
Drexel University
Philadelphia, Pennsylvania 19104
Technical Report AMMRC-TR 81-29, June 1981,
42 pp.-illus.-tables, Contract DAAG46-79-C-0052
D/A Project: 1L162105AH84; AMCMS Code: 612105.H840011
Interim Report, January 1981-April 1981

Unclassified
Unlimited Distribution

Key Words

Filtration
Liquid metals
Aluminum
Steel
Superalloys
Purification

Background on the mechanisms and kinetics of filtration is discussed and the Drexel mathematical model is further elaborated and updated to encompass filtration at the higher temperatures encountered in steels and superalloys. A novel mathematical analysis of inclusion trajectory is also presented. A low temperature model study of liquid inclusion filtration is described and discussed.
The aluminum-TiB$_2$ study has been extended to evaluate a ceramic foam filter.
Reference is made to ongoing work in superalloy and steel filtration, counter-current gas filtration, filter characterization and flow visualization.